

A ruthenium(II) bipyridine complex containing a 4,5-diazafluorene moiety: Synthesis, characterization and its applications in transfer hydrogenation of ketones and dye sensitized solar cells

Akın Baysal^a, Murat Aydemir^{a,b}, Feyyaz Durap^{a,b,*}, Saim Özkar^c, Leyla Tatar Yıldırım^d, Yusuf Selim Ocak^{b,e}

^a Dicle University, Science Faculty, Department of Chemistry, TR-21280 Diyarbakır, Turkey

^b Science and Technology Application and Research Center (DUBTAM), Dicle University, TR-21280 Diyarbakır, Turkey

^c Middle East Technical University, Department of Chemistry, TR-06800 Ankara, Turkey

^d Hacettepe University, Department of Engineering Physics, Beytepe, TR-06800 Ankara, Turkey

^e Dicle University, Faculty of Education, Department of Science, TR-21280 Diyarbakır, Turkey

ARTICLE INFO

Article history:

Received 12 September 2014

Accepted 29 December 2014

Available online 14 January 2015

Keywords:

N ligand

Catalyst

Transfer hydrogenation

DSSC

X-ray

ABSTRACT

The ruthenium(II) complex $[\text{Ru}(\text{bpy})_2\text{L}](\text{PF}_6)_2$, where bpy is 2,2'-bipyridine and **L** is 1,5-dihydro-2-H-cyclopenta[1,2-b:5,4-b']dipyridine-2-one, was synthesized from the reaction of *cis*- $\text{Ru}(\text{bpy})_2\text{Cl}_2 \cdot 2\text{H}_2\text{O}$ with **L**, and isolated as the hexafluorophosphate salt. The structure of **L** was unequivocally elucidated by single-crystal X-ray diffraction analysis. The new ruthenium(II) complex was thoroughly characterized by ^1H and ^{13}C NMR spectroscopy, along with FTIR, UV–Vis and LC MS/MS Triple Quadrupole Mass spectroscopy and elemental analysis. The catalytic activity of $[\text{Ru}(\text{bpy})_2\text{L}](\text{PF}_6)_2$ was tested in the transfer hydrogenation of various ketones in 2-propanol as both the solvent and hydrogen donor. The usage of $[\text{Ru}(\text{bpy})_2\text{L}](\text{PF}_6)_2$ for the formation of a dye sensitized solar cell is also presented.

© 2015 Elsevier Ltd. All rights reserved.

1. Introduction

Ruthenium(II) complexes containing polypyridine ligands have been investigated by many researchers due to their high catalytic performance in homogeneous catalysis [1–3] and high solar power conversion efficiency [4,5]. 4,5-Diazafluorene was reported over four decades ago, but there exist only a few papers reporting the use of 4,5-diazafluorene and its derivatives as ligands in catalytic processes [6]. Jiang and Song [7] have reported the catalytic activity of $[\text{Rh}(\text{cod})(4,5\text{-diazafluorenyl})]$ in the hydrogenation of olefins. The complex has been found to promote the hydrogenation of terminal olefins, though it is not as active as Wilkinson's catalyst [7], without affecting the carbonyl groups in the substrates. $[\text{Rh}(4,5\text{-diazafluorenyl})(\text{PPh}_3)_2(\text{H}_2)\text{Cl}]$ has also been found to be an active catalyst in the hydrogenation of a variety of olefins, including non-terminal ones [8]. Palladium-catalyzed aerobic dehydrogenation in the presence of 4,5-diazafluorene-9-one as a ligand converts aliphatic aldehydes to α,β -unsaturated aldehydes at ambient temperature [9–14].

Transition metal catalyzed transfer hydrogenation is a versatile process for the reduction of multiple bonds to the corresponding saturated compounds due to its easier and safer operation compared to the classical hydrogenation by using molecular hydrogen [15]. Carbonyls are known as one of the most versatile functional groups for organic transformations. A general, mild and direct catalytic route to convert a carbonyl group into the corresponding alcohol would be highly desirable [3]. Over the last two decades, a considerable amount of effort has been devoted to the design and synthesis of new rhodium, ruthenium and iridium complexes bearing C, N, O and P donor ligands for the transfer hydrogenation of ketones [16,17].

Because energy demand and environmental pollution are increasing all over the world, renewable energy sources have become one of the most promising subjects. Among the other renewable energy sources, dye-sensitized solar cells (DSSCs) represent the possibility of low cost and large-scale power production. Ruthenium(II) complexes have been preferred as photosensitizers or dyes in the fabrication of DSSCs. The most commonly used photosensitizers are 2,2'-bipyridine ruthenium(II) (2,2'-bipyridine) complexes with thiocyanate (NCS) ligands, such as *cis*-dithiocyanatobis-(2,2'-bipyridine-4,4'-dicarboxylate)ruthenium(II) (N3 and N719) [18]. Many studies have been performed using NCS free

* Corresponding author at: Department of Chemistry, Dicle University, TR-21280 Diyarbakır, Turkey. Tel.: +90 412 248 8550; fax: +90 412 248 8300.

E-mail address: fdurap@dicle.edu.tr (F. Durap).

complexes for DSSC because NCS is an ambidentate ligand, which can coordinate either at the sulfur or at the nitrogen atom, and is a monodentate ligand, which can be easily replaced [18–22].

Previously, we have designed a series of catalysts containing P-donor ligands, such as aminophosphine, bis(phosphinoamine), phosphinite and aminophosphine-phosphinite, for ketone reduction [23–28]. Herein we report the synthesis and characterization of the $[\text{Ru}(\text{bpy})_2\text{L}](\text{PF}_6)_2$ complex, where bpy is 2,2'-bipyridine and **L** is 1,5-dihydro-2-H-cyclopenta[1,2-b:5,4-b']dipyridine-2-one, as shown in Scheme 1, with the aim of using it as an efficient catalyst in the transfer hydrogenation of ketones.

Our report also includes the construction of a dye sensitized solar cell (DSSC) using the NCS free $[\text{Ru}(\text{bpy})_2\text{L}](\text{PF}_6)_2$ complex as photosensitizer on a nanocrystalline TiO_2 film in light of previous studies reporting efforts to develop new highly efficient sensitizers which can absorb sunlight and inject an electron into the conduction band of nanocrystalline TiO_2 [29–31].

2. Experimental

2.1. Materials

Unless otherwise stated, solvents and materials were used as received and the manipulations were performed in air. *cis*- $\text{Ru}(\text{bipy})_2\text{Cl}_2 \cdot 2\text{H}_2\text{O}$ and 1,5-dihydro-2H-cyclopenta[1,2-b:5,4-b']dipyridine-2-one (**L**) were prepared according to the published procedures [32,33]. NMR spectra were obtained in $\text{DMSO}-d_6$ using a Bruker AV 400 spectrometer. TMS (δ : 0.00 ppm) was used as an internal standard for the ^1H NMR acquisition. A Shimadzu LC MS 8040, LC MS/MS Triple Quadrupole Mass Spectra instrument was used for mass spectra analysis due to its inherent characteristics of accurate mass measurements. UV–Vis spectra were recorded with a Perkin Elmer Lambda 25 spectrometer; FTIR-ATR spectra were recorded with a Perkin Elmer Spectrum 100 spectrometer. The elemental analyses for carbon, hydrogen and nitrogen were carried out on a Costech Combustion System CHNS-O instrument. Analyses by gas chromatography (GC) were performed on a Shimadzu 2010 Plus gas chromatography equipped with a capillary column (5% biphenyl, 95% dimethylsiloxane) (30 m \times 0.32 mm \times 0.25 μm).

2.2. General procedure for the transfer hydrogenation of ketones

A typical procedure for the catalytic hydrogen transfer reaction was as follows: A solution of the complex $[\text{Ru}(\text{bpy})_2\text{L}](\text{PF}_6)_2$, NaOH (0.025 mmol) and the corresponding ketone (0.5 mmol) in degassed *iso*-Pr-OH (5 mL) were refluxed until the completion of

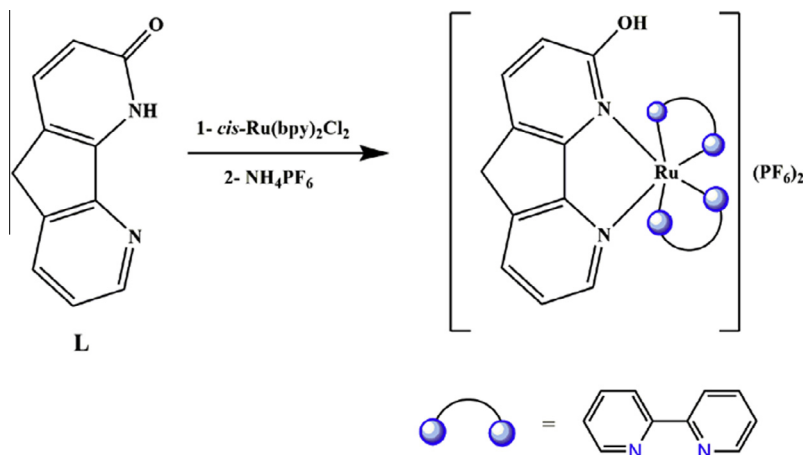
the reaction. After this period, a sample of the reaction mixture was taken, diluted with acetone and analyzed immediately by GC. Conversions obtained were related to the residual unreacted ketone. The GC parameters were as follows: initial temperature, 110 $^\circ\text{C}$; initial time, 1 min; solvent delay, 4.48 min; temperature ramp 80 $^\circ\text{C}/\text{min}$; final temperature, 200 $^\circ\text{C}$; final time, 21.13 min; injector port temperature, 200 $^\circ\text{C}$; detector temperature, 200 $^\circ\text{C}$; injection volume, 2.0 μL .

2.3. Synthesis of $[\text{Ru}(\text{bpy})_2\text{L}](\text{PF}_6)_2$

To a hot solution of the ligand (0.10 g, 0.54 mmol) in ethanol, a solution of *cis*- $\text{Ru}(\text{bipy})_2\text{Cl}_2 \cdot 2\text{H}_2\text{O}$ in the same solvent (5 mL) was added dropwise over 15 min. The mixture was heated to reflux temperature with stirring for 5 h, then the ethanol was removed. The residue obtained was dissolved in a minimum amount of water, then a saturated aqueous solution of $[\text{NH}_4][\text{PF}_6]$ was added dropwise until no more precipitate formed. The mixture was left to stand overnight and filtered. The resulting bright red precipitate was filtered off, dried and recrystallized from ethanol to afford the pure complex (0.48 g, 73%). $\text{C}_{31}\text{H}_{24}\text{N}_6\text{ORuP}_2\text{F}_{12}$ (887.49 g/mol), calcd.: C 41.95, H 2.73, N 9.47; found: C 42.07, H 2.78, N 9.56%. ESI-MS m/z : 597.10 $[\text{M}-2\text{PF}_6]^+$. IR (KBr, cm^{-1}): 3634 (O–H), 1414, 1448 (Aromatic), 829 (PF_6). ^1H NMR (400.1 MHz, $\text{DMSO}-d_6$) δ : {11.96 (br, 1H, OH), 8.81 (m, 3H), 8.73 (d, 1H, $J = 8.1$ Hz), 8.23 (d, 1H, $J = 5.4$ Hz), 8.15–8.19 (m, 4H), 8.05 (t, 2H, $J = 7.82$ Hz), 8.00 (d, 1H, $J = 5.3$ Hz), 7.8 (d, 2H, $J = 5.3$ Hz), 7.63 (t, 1H, $J = 6.3$ Hz), 7.57 (t, 1H, $J = 6.3$ Hz), 7.52 (t, 1H, $J = 6.3$ Hz), 7.44–7.42 (m, 3H), 6.67 (d, 1H, $J = 8.1$ Hz), dipyrindine and aromatic protons}, 4.29 (s, 2H, CH_2); ^{13}C NMR (100.6 MHz, $\text{DMSO}-d_6$) δ : {173.67, 167.75, 166.23, 164.36, 163.44, 163.39, 162.94, 162.24, 161.15, 157.77, 157.06, 153.68, 151.12, 145.67, 143.05, 142.80, 142.61, 142.10, 140.01, 134.05, 133.26, 132.97, 132.67, 131.73, 131.23, 129.39, 128.94, 128.58, 121.40, 117.57, dipyrindine and aromatic carbons}, 41.51 (CH_2); assignment was based on ^1H – ^{13}C HETCOR and ^1H – ^1H COSY spectra. UV–Vis, nm (ϵ , L/mol cm): 243 (24850), 286 (75200), 344 (22100), 428 (12380), 459 (sh) (9730).

2.4. X-ray diffraction structure analysis

X-ray diffraction data were collected on an STOE IPDS 2 two circle diffractometer equipped using graphite-monochromated MoK_α radiation at room temperature. The structure was solved by direct methods and refined using the programs SHELXS97 and SHELXL97 [34] respectively, in the WinGX package [35]. A full-matrix least-squares refinement on F^2 converged at $R = 0.0334$. For all



Scheme 1. Synthesis of $[\text{Ru}(\text{bpy})_2\text{L}](\text{PF}_6)_2$.

non-hydrogen atoms anisotropic displacement parameters were refined. All hydrogen atoms were taken from a difference Fourier map and refined.

2.5. Formation and characterization of DSSC using the $[Ru(bpy)_2L](PF_6)_2$ complex

The DSSC structure was fabricated using a Solaronix test cell titania photoanode. The electrode was sintered at 450 °C in quartz tube furnace for 20 min to remove pollutants, was then cooled to room temperature and immersed in a 1 mM ethanol solution of the Ru complex for 4 h. The titania photoanode was removed from the solution, washed with ethanol and dried with a heat-gun. A Solaronix platinum coated glass cathode was used as a counter electrode and it was fired at 450 °C in a quartz tube furnace for 10 min to reactivate the catalytic platinum layer. The dye coated TiO_2 and Pt electrodes were sealed together with a gasket so that the electrolyte is confined in the cavity. The space left between the two electrodes was filled with an electrolyte (iodide/tri-iodide in a nitrile solvent from Solaronix) that ensures charge transportation through a redox couple. The solar cell area was 0.36 cm². The current–voltage measurements of the sample were performed by means of a Keithley 2400 source meter under a solar Simulator with 100 mW/cm² illumination intensity and an AM1.5 global filter. The results were compared with a reference DSSC structure formed by means of the N719 dye using same fabrication procedures.

3. Results and discussion

3.1. Synthesis and characterization of $[Ru(bpy)_2L](PF_6)_2$

1,5-Dihydro-2H-cyclopenta[1,2-b:5,4-b']dipyridine-2-one, **L**, was prepared in two steps according to the literature procedure [32]. An X-ray quality crystal of **L** was grown from the slow diffusion method in a chloroform-diethyl ether solution. Compound **L** crystallizes in the monoclinic system ($P2_1/c$), including two independent molecules of the formula $C_{11}H_8N_2O$ in the asymmetric

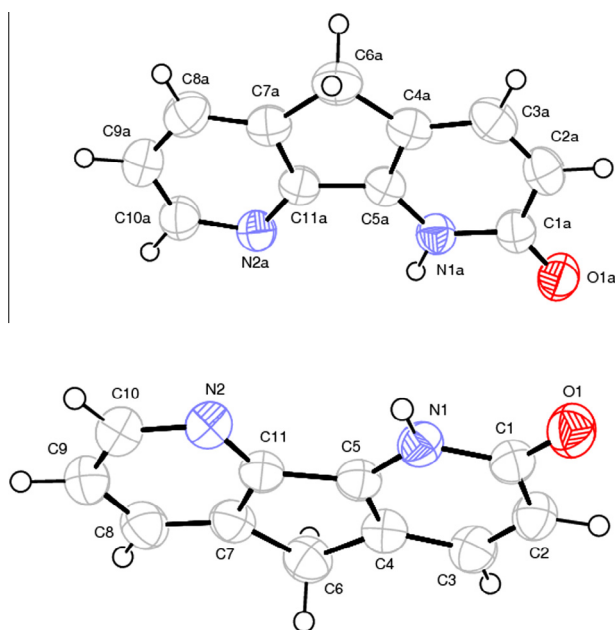


Fig. 1. The molecular structure of 1,5-dihydro-2H-cyclopenta[1,2-b:5,4-b']dipyridine-2-one, (**L**) with the atomic numbering scheme (the crystal structure has two independent molecules in the asymmetric unit).

Table 1

Crystal data and results of the structure refinement for 1,5-dihydro-2H-cyclopenta[1,2-b:5,4-b']dipyridine-2-one, **L**.

Formula	$C_{11}H_8N_2O$
Formula weight (g/mol)	189.19
Temperature (K)	293(2)
Wavelength (Å)	0.71073
Crystal system	monoclinic
Space group	$P2_1/c$
Unit cell dimensions	
<i>a</i> (Å)	10.3155(7)
<i>b</i> (Å)	9.7068(4)
<i>c</i> (Å)	17.7402(13)
β (°)	105.747(13)
Cell volume (Å ³)	1709.67(18)
<i>Z</i>	8
Calculated density [g/cm ³]	1.431
Crystal colour	yellow
Crystal shape	prism
Crystal size (mm)	0.52 × 0.47 × 0.41
<i>F</i> (000)	768
Absorption coefficient (mm ^{−1})	0.095
θ -range for data collection (°)	2.05–27.12
Limiting indices	$-13 \leq h \leq 13$, $-11 \leq k \leq 12$, $-22 \leq l \leq 22$
Reflections collected/unique	3768/2225
Refinement method	Full-matrix least-squares on F^2
Parameters	317
Goodness-of-fit (GOF) on F^2	0.816
Final <i>R</i> indices [$I > 2\sigma(I)$]	$R_1 = 0.0334$, $wR_2 = 0.0658$
Largest difference in peak and hole (e Å ^{−3})	0.128, −0.123

Additional material available from Cambridge Crystallographic Data Center as deposition No: CCDC 1008611 containing H-atom coordinates, thermal parameters and the remaining bond lengths and angles.

Table 2

Selected bond lengths (Å) and angles (°).

O1–C1	1.2448(15)	O1A–C1A	1.2424(15)
N1–C1	1.3736(16)	N1A–C1A	1.3823(17)
N1–C5	1.3629(16)	N1A–C5A	1.3599(16)
N2–C10	1.3470(17)	N2A–C10A	1.3456(17)
N2–C11	1.3344(15)	N2A–C11A	1.3422(16)
C5–N1–C1	121.68(11)	C5A–N1A–C1A	122.22(12)
C11–N2–C10	114.23(12)	C11A–N2A–C10A	114.49(12)
C4–C6–C7	102.52(11)	C4A–C6A–C7A	102.86(11)

unit, with the cell parameters: $a = 10.3155(7)$, $b = 9.7068(4)$, $c = 17.7402(13)$ Å, $\beta = 105.747(13)^\circ$, $V = 1709.67(18)$ Å³ and $Z = 8$. The ORTEP [36] drawing of the molecule is shown in Fig. 1.

The data collection details, crystal data and refinement parameters are listed in Table 1. Selected bond lengths and angles are given in Table 2. Hydrogen bonding and the molecular packing geometry of the ligand molecule was calculated with PLATON [37] and hydrogen bonding geometries are summarized in Table 3.

The two independent molecules in the asymmetric unit are stacked along the *a*/*b*-axis. The two diazafluorenylidene fragments are each nearly planar, excluding the H atoms of the CH₂ group, and are almost parallel each other, the dihedral angle between these planes is 7.79(2)° [38].

The single crystal X-ray structural analysis of the ligand reveals that it has a porous geometry which is stabilized by intermolecular interactions of both hydrogen-bonds and stacking between the diazafluorene moieties (Fig. 2).

The molecular packing in the solid state is porous structure along the *c*-axis, as shown in Fig. 3a, where green and blue colours represent M1 and M2, respectively. Some special distances of the packing are given in Fig. 3b.

A cationic ruthenium(II) complex was prepared by the reaction of 1,5-dihydro-2H-cyclopenta[1,2-b:5,4-b']dipyridine-2-one (**L**)

Table 3

Structural parameters of the hydrogen bonds between the donor (D), acceptor (A) and hydrogen (H).

D–H...A	D–H (Å)	A...H (Å)	D...A (Å)	D–H...H (°)
N1–H1...N2A ⁱ	0.900(16)	2.329(16)	3.1999(16)	162.9(13)
N1A–H1A...O1 ⁱⁱ	0.952(17)	1.788(17)	2.7274(15)	168.5(14)
C3–H3...O1 ⁱⁱⁱ	1.006(15)	2.278(15)	3.2705(17)	169.0(12)
C8A–H8A...O1A ^{iv}	0.957(15)	2.572(15)	3.3896(19)	143.5(12)
C10A–H10A...N2 ⁱⁱ	1.002(15)	2.574(15)	3.5495(19)	164.4(11)

Symmetry codes [i: x, 1 + y, z; ii: x, –1 + y, z; iii: 1 – x, –1/2 + y, 1/2 – z; iv: x, 1/2 – y, –1/2 + z].

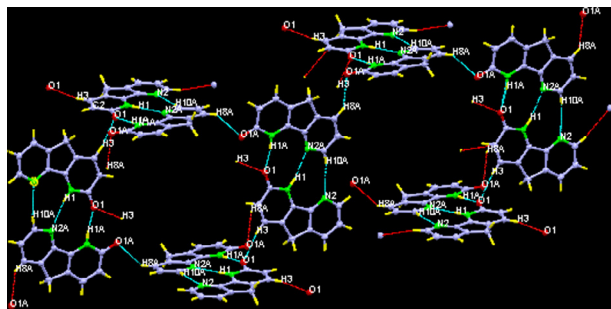
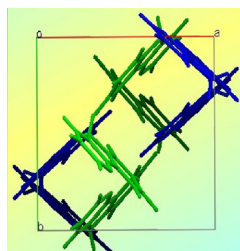
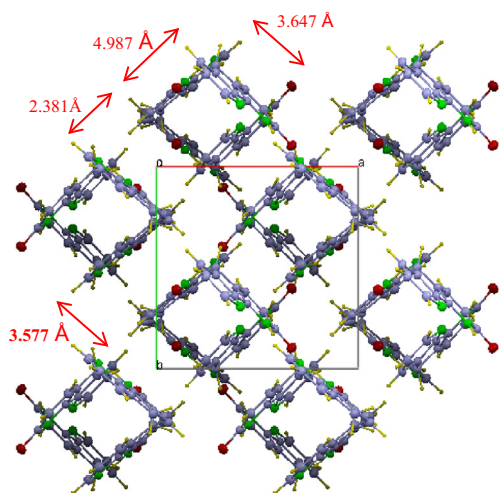


Fig. 2. Stacking geometry and details of the distances in the crystal structure of 1,5-dihydro-2H-cyclopenta[1,2-b:5,4-b']dipyridine-2-one, **L** [38].



(a)



(b)

Fig. 3. Molecular packing geometry of the structure along the c-axis [38].

with *cis*-dichlorobis(2,2'-bipyridine) ruthenium(II) in ethanol. The ruthenium(II) complex was isolated as the analytically pure hexafluorophosphate salt, [Ru(bpy)₂L](PF₆)₂, where **L** is the enol form of 1,5-dihydro-2H-cyclopenta[1,2-b:5,4-b']dipyridine-2-one (Fig. 4 and Scheme 1).

The red complex [Ru(bpy)₂L](PF₆)₂ was characterized by ¹H and ¹³C NMR, FTIR, LC–MS, UV–Vis and elemental analysis (for details

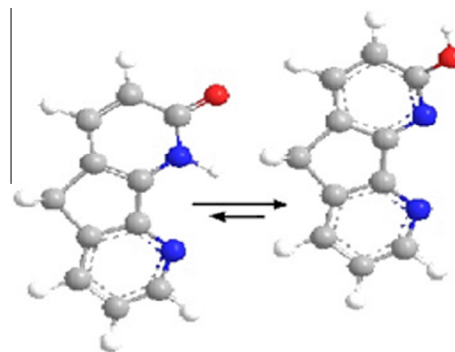


Fig. 4. Keto-enol form of 1,5-dihydro-2H-cyclopenta[1,2-b:5,4-b']dipyridine-2-one, **L**.

Table 4

Transfer hydrogenation of acetophenone with *iso*-PrOH, catalyzed by [Ru(bpy)₂L](PF₆)₂.

Entry	S/Cat./NaOH	Time (h)	Conversion (%) ^d	TOF (h ^{−1}) ^e
1	100:1:5 ^a	24	Trace	–
2	100:1 ^b	48	<3	–
3	100:1:5 ^c	4	99	25

Reaction conditions:

^a At room temperature; acetophenone/Cat./NaOH, 100:1:5.

^b Refluxing in *iso*-PrOH; acetophenone/Cat. 100:1, in the absence of base.

^c Refluxing in *iso*-PrOH; acetophenone/Cat./NaOH, 100:1:5.

^d Determined by GC (three independent catalytic experiments).

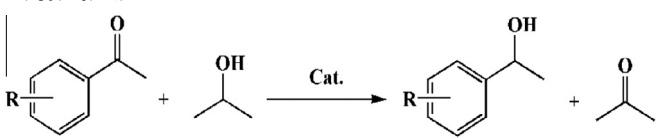
^e Referred at the reaction time indicated in column; TOF = (mol product/mol Cat.) × h^{−1}.

see experimental section). The ¹H NMR spectrum of the complex shows peaks for the protons of both ligands. It is noteworthy that the observation of a broad ¹H NMR signal at δ(H) 11.96 ppm is due to the hydroxyl H-atom. This suggests that the OH group in the ligand **L** does not participate in metal binding. Compared with the IR spectrum of the ligand, the band at 1651 cm^{−1} due to ν(CO) in the ligand **L** disappeared upon complex formation. The weak absorption at 3634 cm^{−1} is attributed to ν(O–H) in the complex. The disappearance of a sharp signal at 1651 cm^{−1} and the appearance of new broad band at 3634 cm^{−1} in the IR spectrum and a broad signal at 11.96 ppm in the ¹H NMR spectrum indicate the isomerisation of the C=O group to its enol form with the involvement of the NH group prior to complex formation. The presence of the PF₆[−] group in the complex is also evident from the IR absorption band at 829 cm^{−1}. In the electron spray ionization mass spectrum of the complex, a signal for the complex cation [M–2PF₆]⁺ was observed at *m/z* 597.10 for the complex, consistent with the expected value.

The electronic absorption spectrum of complex in methanol is mainly dominated by absorptions at 243, 286 and 344 nm, and a weak low energy band at 428 nm together with a shoulder at 459 nm, typical of ruthenium(II) tris(bipyridine) derivatives [39], with reference to earlier studies on related ruthenium(II) polypyridine systems [40]. The higher energy absorption bands are attributed to intra ligand transitions, while the low energy bands are assigned to metal-to-ligand charge transfer transitions, which are not observed in the electronic absorption spectrum of the free ligand.

Table 5

Transfer hydrogenation results for substituted acetophenones with the catalyst $[\text{Ru}(\text{bpy})_2\text{L}](\text{PF}_6)_2$.^a



Entry	R	Time (h)	Conversion (%) ^b	TOF (h ⁻¹) ^c
1	4-F	3	98 ± 1	33
2	4-Cl	4	98 ± 1	25
3	4-Br	4	99 ± 0.5	25
4	4-NO ₂	3	99 ± 0.5	33
5	4-Me	9	97 ± 2	11
6	2-MeO	7	99 ± 0.5	14
7	4-MeO	10	98 ± 1	<10

Reaction conditions:

^a Catalyst (0.005 mmol), substrate (0.5 mmol), *iso*-PrOH (5 mL), NaOH (0.025 mmol), 82 °C, the concentration of the acetophenone derivatives is 0.1 M.

^b The purity of the compounds was checked by ¹H NMR and GC (three independent catalytic experiments), yields are based on aryl ketone.

^c TOF = (mol product/mol Cat.) × h⁻¹.

3.2. Catalytic studies

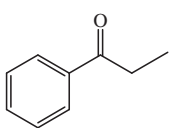
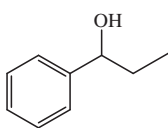
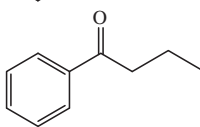
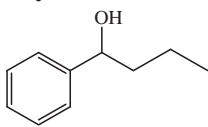
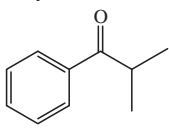
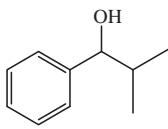
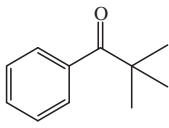
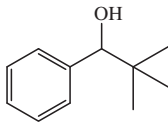
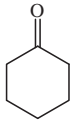
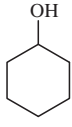
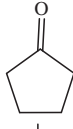
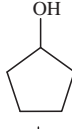
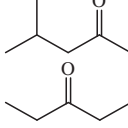
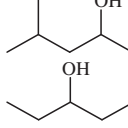
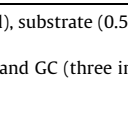
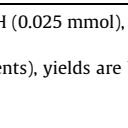
In a preliminary study, we examined the transfer hydrogenation of acetophenone to produce 1-phenylethanol using the complex

$[\text{Ru}(\text{bpy})_2\text{L}](\text{PF}_6)_2$ as a catalyst in 2-propanol both as a solvent and hydrogen source. Initially, to an *iso*-PrOH solution of the Ru(II) complex, an appropriate amount of acetophenone and NaOH/*iso*-PrOH solution were added at room temperature (acetophenone/Cat./NaOH; 100:1:5 M ratios). At room temperature no noticeable formation of 1-phenylethanol was observed (Table 4, entry 1). A blank experiment was performed to demonstrate that the transfer hydrogenation does not occur in the absence of catalyst. The catalytic activity of the complex is improved by increasing the reaction temperature to 82 °C (Table 4, entry 3). As seen in Table 4, the complex is very active, leading to a quantitative transformation of the acetophenone with a complex/NaOH ratio of 1:5 at 82 °C. Furthermore, as can be inferred from Table 4 (entry 2), the presence of base (NaOH) is necessary to observe an appreciable conversion. The base most likely facilitates the formation of ruthenium alkoxide by abstracting the proton of the alcohol and subsequently the alkoxide undergoes β-elimination to give hydride, which is an active species in this reaction [41,42]. The results of the optimization studies showed clearly that excellent conversions were achieved in the reduction of acetophenone to 1-phenylethanol when the complex $[\text{Ru}(\text{bpy})_2\text{L}](\text{PF}_6)_2$ was used as a catalytic precursor with a substrate to catalyst molar ratio of 100:1 at reflux temperature in *iso*-PrOH (Table 4).

After optimization of the reaction conditions, we also examined acetophenone derivatives as substrates for transfer hydrogenation using the $[\text{Ru}(\text{bpy})_2\text{L}](\text{PF}_6)_2$ complex in 2-propanol. A variety of

Table 6

Transfer hydrogenation results for substituted alkyl phenyl ketones with the catalyst.

Entry	Time (h)	Substrate	Product	Conversion (%) ^a
1	5			98 ± 1
2	7			99 ± 0.5
3	8			98 ± 1
4	12			97 ± 2
5	4			98 ± 1
6	4			97 ± 1
7	7			98 ± 0.5
8	9			96 ± 1

Reaction conditions: $[\text{Ru}(\text{bpy})_2\text{L}](\text{PF}_6)_2$ catalyst (0.005 mmol), substrate (0.5 mmol), *iso*-PrOH (5 mL), NaOH (0.025 mmol), 82 °C, the concentration of alkyl phenyl ketones is 0.1 M.

^a The purity of the compounds was checked by ¹H NMR and GC (three independent catalytic experiments), yields are based on aryl ketone.

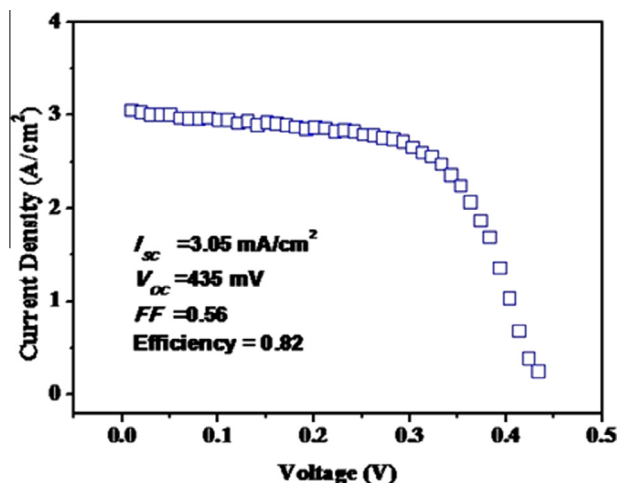


Fig. 5. Current density–voltage measurement of the DSSC structure.

simple ketones (substrate/catalyst = 100:1) can be transformed into their corresponding secondary alcohols with high conversions, as illustrated in Table 5. An examination of the catalytic activity of $[\text{Ru}(\text{bpy})_2\text{L}](\text{PF}_6)_2$ showed that it is an efficient catalyst affording almost quantitative transformation of the ketones within a short time (Table 5). As expected, the electronic properties (the nature and position) of the substituents on the phenyl ring of the ketone caused the changes in the extent of reduction. To ensure that the observed results could be attributed to purely electronic effects [43–45], para- and ortho-substituted acetophenone derivatives were tested for transfer hydrogenation. The results indicated that strong electron withdrawing substituents, such as F, NO_2 and Cl, speed up the reaction (Table 5). Conversely, the most electron-donating substituents, (2- or 4-methoxy) led to lower conversions. It is well-known that the presence of an electron withdrawing group can ease hydrogen transfer reactions [46,47], which has been attributed to the hydridic nature of the reducing species involved. As such, substrates with fluoro or nitro groups undergo higher conversions owing to rapid hydride transfer, while substrates with electron-donating substituents (2- or 4-methoxy) undergo a slower reaction in a more controlled manner [48,49]. The results indicate that high conversions were achieved in the reduction of acetophenone derivatives when $[\text{Ru}(\text{bpy})_2\text{L}](\text{PF}_6)_2$ was used as the catalyst precursor.

We also carried out further experiments to investigate the effect of the bulkiness of the alkyl groups on the catalytic activity and the results were given in Table 6. A variety of simple aryl alkyl ketones were transformed to the corresponding secondary alcohols. It was observed that the activity is considerably dependent on the steric hindrance of the alkyl group. The reactivity is gradually reduced by increasing the bulkiness of the alkyl groups [45–49]. Prompted by the high catalytic activities obtained in these studies, we next extended our studies to include hydrogenation of various simple ketones. An investigation of the catalytic activity of $[\text{Ru}(\text{bpy})_2\text{L}](\text{PF}_6)_2$ showed that it is an effective catalyst, enabling almost quantitative transformation of the ketones in short times (Table 6).

3.3. Photovoltaic properties of DSSC based on $[\text{Ru}(\text{bpy})_2\text{L}](\text{PF}_6)_2$

The current voltage measurements of the DSSC structure formed using the Ru complex are presented in Fig. 5. The open circuit photovoltage (V_{OC}) and short circuit photocurrent density (J_{SC}) are determined as 435 mV and 3.05 mA/cm^2 from Fig. 5, respectively. Using the V_{OC} and J_{SC} values, the fill factor (FF) and solar to electricity conversion efficiency (η) were calculated as 0.56% and 0.82%, respectively. The V_{OC} , J_{SC} , FF and η of the reference solar cell fabri-

cated using the N719 photosensitizer were evaluated as 720 mV, 25.74 mA/cm^2 , 0.45% and 8.15%, respectively. The lower power conversion efficiency can be attributed the weaker binding of $[\text{Ru}(\text{bpy})_2\text{L}](\text{PF}_6)_2$ to TiO_2 with respect to the N719 dye. Zalas et al. [50] synthesized a new dinuclear dendritic-like ruthenium dye which consists of two trisbipyridyl ruthenium(II) derivatives clipped with an ethyl 3,5-diethynylbenzoate group. They have presented spectroscopic and electrochemical characterization of the new compound and used it in the fabrication of a DSSC. They have reported that the solar cell formed using the new dinuclear dendritic-like ruthenium dye had 60.5% FF and 0.32% photon-to-current conversion efficiency values. Furthermore, Pellegrin et al. [51] obtained ruthenium polypyridine complexes as sensitizers in NiO based p-type dye-sensitized solar cells and analyzed the effects of the anchoring groups. They determined the efficiency of the solar cells as being between 0.0065 and 0.025%. The FF values of the cells were about 0.34% for all samples. Therefore, it can be said that the efficiency of the cell based on $[\text{Ru}(\text{bpy})_2\text{L}](\text{PF}_6)_2$ is satisfying on comparison with cells formed using similar compounds.

4. Conclusions

In the present study, the cationic Ru(II) complex $[\text{Ru}(\text{bpy})_2\text{L}]^{2+}$ was synthesized in high yield by the reaction of *cis*- $\text{Ru}(\text{bpy})_2\text{Cl}_2 \cdot 2\text{H}_2\text{O}$ with 1,5-dihydro-2H-cyclopenta[1,2-b:5,4-b']dipyridine-2-one, **L**. The crystal structure of **L** was also determined by single crystal X-ray diffraction. The $[\text{Ru}(\text{bpy})_2\text{L}](\text{PF}_6)_2$ complex was found to be a highly active homogeneous catalyst in the reduction of various ketones via hydrogen transfer from 2-propanol and readily lead to secondary alcohols in high yields. In addition, a dye sensitized solar cell based on the $[\text{Ru}(\text{bpy})_2\text{L}](\text{PF}_6)_2$ complex with 0.82% solar conversion efficiency is reported.

Acknowledgements

Partial support from the Dicle University Research Fund (Project Nos. 02-FF-33, DÜBAP-14-FF-75) and the Turkish Academy of Sciences is gratefully acknowledged. The analysis was conducted at Dicle University Science and Technology Application and Research Center (DUBTAM). The authors thank Canan Kazak for the X-ray single crystal data collection.

Appendix A. Supplementary data

CCDC 1008611 contain the supplementary crystallographic data for 1,5-dihydro-2-H-cyclopenta[1,2-b:5,4-b']dipyridine-2-one. These data can be obtained free of charge via <http://www.ccdc.cam.ac.uk/conts/retrieving.html>, or from the Cambridge Crystallographic Data Centre, 12 Union Road, Cambridge CB2 1EZ, UK; fax: (+44) 1223-336-033; or e-mail: deposit@ccdc.cam.ac.uk.

References

- [1] S.A. Moya, M. Vidal, G. Abarca, C. Martinez, V. Guerchais, H. Le Bozec, M.T. Garland, S. Rodriguez, P. Aguirre, *Inorg. Chem. Commun.* 13 (2010) 1519.
- [2] S.A. Moya, M. Vidal, K. Brown, C. Negrete-Vergana, G. Abarca, P. Aguirre, *Inorg. Chem. Commun.* 22 (2012) 146.
- [3] P. Stepnicka, J. Ludvik, J. Canivet, G. Süß-fink, *Inorg. Chim. Acta* 359 (2006) 2369.
- [4] D. Martineau, M. Beley, P.C. Gros, S. Cazzanti, S. Caramori, C.A. Bignozzi, *Inorg. Chem.* 46 (2007) 2272.
- [5] D. Martineau, M. Beley, P.C. Gros, *J. Org. Chem.* 71 (2) (2006) 566.
- [6] K. Kloc, J. Mlochowski, Z. Szule, *Heterocycles* 9 (1978) 849.
- [7] H. Jiang, D. Song, *Organometallics* 27 (2008) 3587.
- [8] H. Jiang, E. Stepowska, D. Song, *Eur. J. Inorg. Chem.* (2009) 2083.
- [9] W. Gao, Z. He, Y. Qian, J. Zhao, Y. Huang, *Chem. Sci.* 3 (2012) 883.
- [10] M. Piotrowicz, J. Zakrzewski, *Organometallics* 32 (2013) 5709.
- [11] A.N. Campbell, S.S. Stahl, *Acc. Chem. Res.* 45 (2012) 851.
- [12] T.N. Diao, J.J. Wadzinski, S.S. Stahl, *Chem. Sci.* 3 (2012) 887.

- [13] A.N. Campbell, P.B. White, I.A. Guzei, S.S. Stahl, J. Am. Chem. Soc. 132 (2010) 15116.
- [14] A. Kilic, F. Durap, M. Aydemir, A. Baysal, E. Tas, J. Organomet. Chem. 693 (2008) 2835.
- [15] Y. Himeda, N. Onozawa-Komatsuzaki, H. Sugihara, H. Arakawa, K. Kasuga, J. Mol. Catal. A: Chem. 195 (2003) 95.
- [16] H. Türkmen, İ. Kani, B. Çetinkaya, Eur. J. Inorg. Chem. (2012) 4494.
- [17] O. Dayan, N. Özdemir, Z. Şerbetçi, M. Dinçer, B. Çetinkaya, Inorg. Chim. Acta 392 (2012) 246.
- [18] C. Dragonetti, A. Valore, A. Colombo, D. Roberto, V. Trifiletti, N. Manfredi, M.M. Salamone, R. Ruffo, A. Abbotto, J. Organomet. Chem. 714 (2012) 88.
- [19] K.C.D. Robson, B.D. Koivisto, A. Yella, B. Sporinova, M.K. Nazeeruddin, T. Baumgartner, M. Gratzel, C.P. Berlinguette, Inorg. Chem. 50 (2011) 5494.
- [20] C. Dragonetti, A. Colombo, M. Magni, P. Mussini, F. Nisic, D. Roberto, R. Ugo, A. Valore, A. Valsecchi, P. Salvatori, M.G. Lobello, F.D. Angelis, Inorg. Chem. 52 (2013) 10723.
- [21] T. Bessho, E. Yoneda, J.H. Yum, M. Guglielmi, I.T.H. Imai, U. Rothlisberger, M.K. Nazeeruddin, M. Gratzel, J. Am. Chem. Soc. 131 (2009) 5930.
- [22] S.H. Wadman, J.M. Kroon, K. Bakker, R.W.A. Havenith, G.P.M. van Klink, G.V. Koten, Organometallics 29 (2010) 1569.
- [23] M. Aydemir, N. Meriç, A. Baysal, J. Organomet. Chem. 720 (2012) 38.
- [24] C. Kayan, N. Meriç, M. Aydemir, Y.S. Ocak, A. Baysal, H. Temel, Appl. Organomet. Chem. 28 (2014) 127.
- [25] F. Ok, M. Aydemir, F. Durap, A. Baysal, Appl. Organomet. Chem. 28 (2014) 38.
- [26] F. Durap, M. Aydemir, D. Elma, A. Baysal, Y. Turgut, C. R. Chimie 16 (2013) 363.
- [27] F. Durap, M. Aydemir, A. Baysal, D. Elma, B. Ak, Y. Turgut, Inorg. Chim. Acta 411 (2014) 77.
- [28] N. Meric, F. Durap, M. Aydemir, A. Baysal, Appl. Organomet. Chem. 28 (2014) 803.
- [29] Y. Hou, D. Wang, X.H. Yang, W.Q. Fang, B. Zhang, H.F. Wang, H.G. Yang, Nat. Commun. 4 (2013) 1583.
- [30] X. Yin, Z. Xue, L. Wang, Y. Cheng, B. Liu, ACS Appl. Mater. Inter. 4 (3) (2012) 1709.
- [31] Y. Yu, K. Wu, K. Shen, K.D. Wang, Eur. Phys. J. Appl. Phys. 61 (01) (2013) 10201.
- [32] A. Baysal, F. Durap, B. Gümgüm, L.T. Yıldırım, D. Ülkü, A.D. Boğa, S. Özkar, Helv. Chim. Acta 90 (2007) 1211.
- [33] B.P. Sullivan, D.J. Salmon, T.J. Meyer, Inorg. Chem. 17 (1978) 3334.
- [34] G.M. Shelx, Sheldrick, Acta Cryst. A 64 (2008) 112.
- [35] G.X. Win, L.J. Farrugia, J. Appl. Cryst. 32 (1999) 837.
- [36] ORTEP 3: L.J. Farrugia, J. Appl. Cryst. 30 (1997) 565.
- [37] PLATON: A.L. Spek, Acta Cryst. D65 (2009) 148.
- [38] MERCURY: C.F. Macrae, P.R. Edgington, P. McCabe, E. Pidcock, G.P. Shields, R. Taylor, M. Towler, J. van de Streek, J. Appl. Cryst. 39 (2006) 453.
- [39] I.K. Shoen, E.B. Amy, D.S. Gregory, S. Milan, M.G. Mark, Inorg. Chem. 38 (1999) 2411.
- [40] A. Juris, U. Balzani, F. Barigelli, S. Campagna, P. Belser, A. Von Zelewsky, Coord. Chem. Rev. 84 (1988) 85.
- [41] H. Doucet, T. Ohkuma, K. Murata, T. Yokozawa, M. Kozawa, E. Katayama, F.A. England, T. Ikariya, R. Noyori, Angew. Chem. Int. Ed. 37 (1998) 1703.
- [42] H. Zhang, B.C. Yang, Y.Y. Li, Z.R. Dong, J.X. Gao, H. Nakamura, K. Murata, T. Ikariya, J. Chem. Com., Chem. Commun. (2003) 142.
- [43] R. Guo, X.H. Chen, C. Elphelt, D. Song, R.H. Morris, Org. Lett. 7 (2005) 1757.
- [44] P. Pelagatti, M. Carcelli, F. Calbiani, C. Cassi, L. Elviri, C. Pelizzi, U. Rizzotti, D. Rogolino, Organometallics 24 (2005) 5836.
- [45] J.W. Faller, A.R. Lavoie, Organometallics 20 (2001) 5245.
- [46] J.-X. Gao, X.-D. Yi, P.-P. Xu, C.-L. Tang, H.-L. Wan, T. Ikariya, J. Organomet. Chem. 592 (1999) 290.
- [47] J.-X. Gao, H. Zhang, X.-D. Yi, P.-P. Xu, C.-L. Tang, H.-L. Wan, K.-R. Tsai, T. Ikariya, Chirality 12 (2000) 383.
- [48] J.-S. Chen, Y.-Y. Li, Z.-R. Dong, B.-Z. Li, J.-X. Gao, Tetrahedron Lett. 45 (2004) 8415.
- [49] Z.-R. Dong, Y.-Y. Li, J.-S. Chen, B.-Z. Li, Y. Xing, J.-X. Gao, Org. Lett. 7 (2005) 1043.
- [50] M. Zalas, B. Gierczyk, M. Klein, K. Siuzdak, T. Pędziński, T. Łuczak, Polyhedron 67 (2014) 381.
- [51] Y. Pellegrin, L. Le Pleux, E. Blart, A. Renaud, B. Chavillon, N. Szuwarski, F. Odobel, J. Photochem. Photobiol. A: Chem. 219 (2) (2011) 235.